멤브레인(Membrane Journal)
Vol. 34 No. 5 October 2024, 241-252

총 설

Print ISSN: 1226-0088
Online ISSN: 2288-7253
DOI: https://doi.org/10.14579/MEMBRANE_JOURNAL.2024.34.5.241

미세다공성 분리막의 기공특성 분석법

박 인 호 · 강 준 혁 · 박 호 범†

한양대학교 에너지공학과

(2024년 10월 10일 접수, 2024년 10월 18일 수정, 2024년 10월 18일 채택)

Pore Characterization Methods for Microporous Membranes

Inho Park, Jun Hyeok Kang, and Ho Bum Park†

Department of Energy Engineering, Hanyang University, Seoul 04763, Korea

(Received October 10, 2024, Revised October 18, 2024, Accepted October 18, 2024)

요 약: 분리막 공정 설계에 있어 응용 분야에 적합한 막 소재 및 물성 선택은 중요하다. 특히 다공성 막의 경우, 분리 메커니즘이 투과 종 크기에 따라 선별되는 원리에 기반함에 따라 기공 크기와 같은 기공 특성을 확인하는 막 소재 스크리닝이 우선되어야 한다. 하지만 일반적으로 분리막 매질 내의 기공들은 불균일하게 형성된다. 본 논문에서는 이러한 불균일성을 정규화한 기공 크기 분포도 분석 기법들에 대해 중점적으로 다루고 각 기법들이 기반한 Young-Laplace, Kelvin 그리고 Gibbs-Thomson 식에 대해 소개하고자 한다.

Abstract: Selecting an appropriate membrane for a given application is essential. In microporous membranes, the separation mechanism relies on size exclusion, meaning that the pore size determines which substances can permeate. Therefore, pore characterization techniques are employed beforehand to identify the most suitable material. However, pore geometry and tortuosity are typically random within the membrane matrix. This paper reviews indirect methods for characterizing pore size distribution, utilizing three key equations—the Young-Laplace, Kelvin, and Gibbs-Thomson equations—to account for the random nature of the pores.

Keywords: *microporous membrane, porometry, pore size distribution, wetting fluid, microfiltration, ultrafiltration*

1. Introduction

Membrane processes consume less energy compared to traditional separation methods, require less operational space, and generate fewer by-products, making them efficient and environmentally friendly[1-3]. Additionally, membrane technology has a wide range of applications, including gas separation, organic solvent separation, seawater desalination, packaging, and pharmaceuticals. The choice of membrane material depends on the type of substance to be separated. While several factors, such as chemical resistance and cost-effectiveness, must be considered when selecting membrane materials, the pore characteristics of the membrane are generally the primary determinant of which species permeate or are retained in a mixture.

Membranes are broadly classified into porous and non-porous types based on pore size. Non-porous membranes, used in applications such as gas separation, reverse osmosis, and pervaporation, exhibit pore structures that dynamically change according to the diffusion behavior of the permeating species. This can be explained by the solution-diffusion model. On the other hand, while porous membranes maintain their physical

†Corresponding author(e-mail: badtzhb@hanyang.ac.kr; http://orcid.org/0000-0002-8003-9698)

pore structure regardless of the diffusion behavior of the permeating species, there is no single comprehensive model that describes them. The pore-flow model, which explains the behavior of substances based on pressure gradients through fine pores, may or may not apply depending on the characteristics of the porous membrane.

Given these factors, the analysis techniques used to interpret and cross-verify the separation performance of porous membranes become crucial. In general, the separation mechanism of porous membranes involves molecular sieving, where only species small enough to physically pass through the pores can permeate. The pore characteristics as molecular sieves include not only pore size but also pore size distribution (PSD), porosity, tortuosity, and connectivity. Each of these characteristics requires different analytical methods. This paper focuses on methods for analyzing pore size distribution, one of the key characteristics of porous membranes.

2. Main Discussion

2.1. Types of porous membranes

As shown in Fig. 1, porous membranes can be classified into two types based on their structure: screen filters and depth filters. Screen filters have finely structured surface pores that filter particles at the membrane surface. These membranes exhibit an asymmetric structure, composed of a surface layer with small pores and a support layer with relatively larger pores, and are typically used in ultrafiltration membranes (pore size: 2~100 nm). This indicates that screen filters are suitable for filtering fluids with a relatively narrow particle size distribution. The filtration mechanism of screen filters can be explained using the Ferry-Renkin equation (Equation 1), which accounts for the pore size (r), the particle size (a), and the parabolic velocity profile of the fluid as it passes through the pores[4,5].

$$R = \left[1 - 2\left(1 - \frac{a}{r}\right)^2 + \left(1 - \frac{a}{r}\right)^4\right] \times 100\% \quad (1)$$

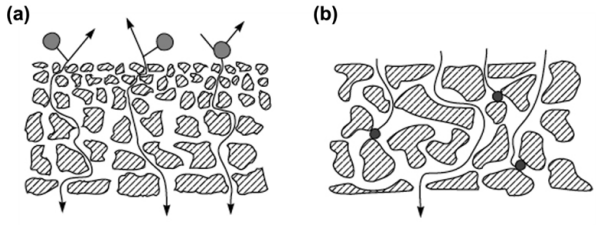

Fig. 1. Classification of microporous membranes – (a) surface filtration, (b) depth filtration (reproduced with permission from [3]).

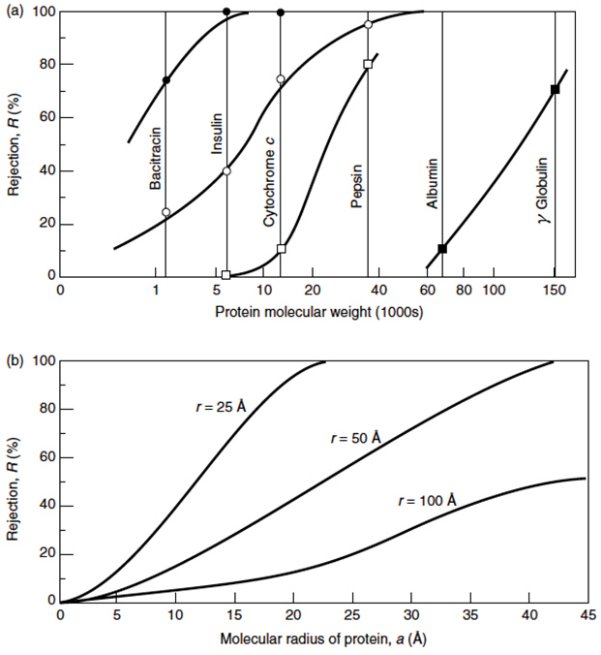

Fig. 2. (a) Rejection of microfiltration with respect to globular protein molecular weight, (b) theoretical correlation between molecular radius and pore radius using Ferry-Renkin equation (reproduced with permission from [3,5]).

Equation 1 is used to estimate the pore size of the membrane based on the radius of the filtrate particles and the membrane rejection rate (R). In Fig. 2(a), an example is provided where the equation is applied to actual spherical proteins, plotting a rejection rate curve for the membrane. Spherical proteins were chosen as marker proteins because their simple shape allows for the calculation of particle size based solely on molecular weight. In Fig. 2(b) curve indicates the rejection as a function of the radius of the protein at a fixed pore size.

Depth filters, on the other hand, allow particles to pass through the membrane thickness, where filtration occurs within the membrane structure. Unlike screen filters, depth filters have a symmetric structure and are typically used in microfiltration membranes (pore size: 100~500 nm). The filtration mechanism of depth filters includes not only size sieving, where particles are filtered based on their size as they pass through the membrane, but also adsorption of particles within the membrane structure. The filtration mechanisms can be further categorized as follows: 1) size sieving, where particles are filtered based on size; 2) inertial capture, where larger particles are trapped against the membrane wall due to their inability to follow the fluid flow; 3) adsorption due to Brownian diffusion, where smaller particles adhere to the membrane surface due to irregular motion; and 4) electrostatic adsorption, where charged particles are captured based on the electrostatic properties of the membrane. Depth filters are suitable for filtering fluids with a wide range of particle size distributions, but in cases where electrostatic adsorption is used, the rejection rate may decrease if the membrane's charge performance deteriorates over time.

2.2. Types of pore characteristics to consider

In porous membranes, pore characteristics are directly linked to separation performance, making their determination and analysis crucial. However, the values associated with these characteristics may not always accurately represent membrane performance. As shown in Fig. 3(a), even if the average porosity of a screen filter membrane is 0.7~0.8, the porosity of the actual filtering layer (skin layer) may be as low as 0.05, significantly lower than the average. Additionally, porous membranes with a range of pore sizes have different standards for defining representative pore size, depending on the membrane type (See Fig. 3(b)). For ultrafiltration membranes, the mean pore size is typically used as the representative value, while for microfiltration membranes, the size of the largest particles that can permeate is used as the representative pore

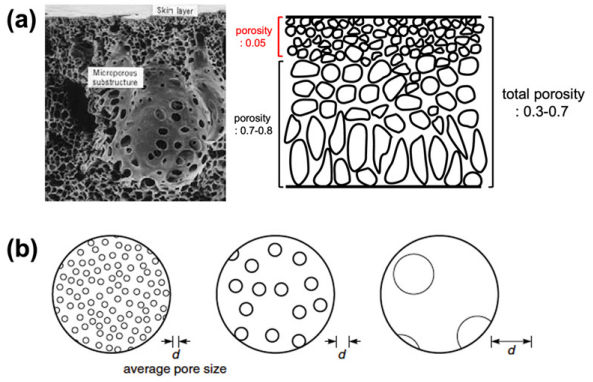

Fig. 3. (a) Example of asymmetric membrane porosity, (b) porous membrane pore characteristic based on mean pore size (reproduced with permission from [3]).

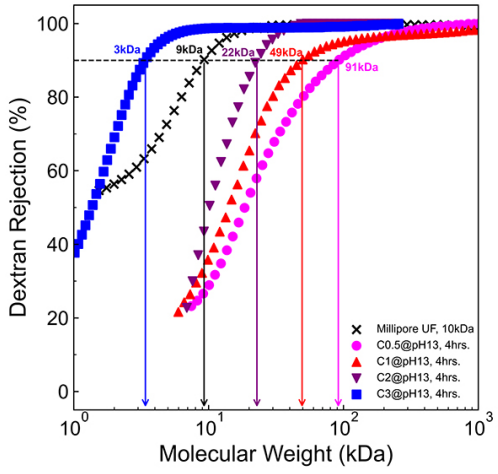

Fig. 4. Molecular weight cut-off curve (reproduced with permission from [7]).

size. Consequently, the actual measured pore size for microfiltration membranes is often significantly smaller than the representative value.

A common indicator used as a substitute for pore characteristics is the molecular weight cutoff (MWCO). By gradually increasing the molecular weight of a substance and passing it through the membrane, an S-shaped curve can be obtained, showing the relationship between molecular weight and rejection rate (Fig. 4). The molecular weight at which the rejection rate reaches 90% is referred to as the MWCO of the membrane, and it is often used to assess the pore characteristics of ultrafiltration membranes.

However, MWCO cannot be considered an absolute

indicator for several reasons[6]. First, the MWCO value can vary depending on the choice of marker protein, as the shape and size of proteins, even with the same molecular weight, can differ under test conditions. Second, the wide variance in pore size distribution of ultrafiltration membranes can make it difficult to precisely define the MWCO. Third, even for the same membrane, MWCO values can vary depending on how test conditions such as pressure and measurement time are set by the tester. Fourth, since ultrafiltration membranes are generally hydrophobic, proteins may adsorb onto the membrane surface or interior, and the extent of this adsorption can vary depending on factors like protein concentration, solvent pH, and ionic strength. If these variables are not controlled, the membrane's rejection rate or MWCO may not reflect its true performance. Therefore, it is crucial for testers to control the testing conditions and environment to accurately determine the MWCO, allowing for meaningful comparisons of membrane characteristics.

2.3. Analysis methods and theories for pore characteristics

Methods for analyzing the pore characteristics of porous membranes can be categorized into direct and indirect approaches. Direct methods, such as scanning electron microscopy (SEM), transmission electron microscopy (TEM), and atomic force microscopy (AFM), allow for the observation of the membrane's surface and cross-sectional morphology[8-10]. These techniques provide real-time direct visualization of surface porosity, pore shape, and pore size. However, their limitation lies in their localized analysis, which requires a large number of samples to obtain representative data for the entire membrane.

In contrast, indirect methods infer pore size distribution based on theoretical models and measurement data. Indirect approaches can be further divided into three categories according to the underlying theory:

1) Methods based on the Young-Laplace equation, such as the bubble point method and liquid displacement method.

2) Techniques based on the Kelvin equation, including permoporometry, gas adsorption-desorption, and evapoporometry.

3) Methods based on the Gibbs-Thomson equation, such as thermoporometry.

This mini review focuses on how these theoretical models are applied to various analytical techniques and how each method is utilized for characterizing porous membranes.

2.3.1. Young-laplace equation

The Young-Laplace equation describes the pressure gradient across the interface between two immiscible fluids and is commonly used to interpret surface tension in capillary phenomena. Assuming the pores of the membrane are cylindrical in shape and the interface of two immiscible fluids (e.g., gas-liquid or liquid-liquid) is distributed within these pores, the pressure difference (△p) across the interface can be expressed as follows:

$$\triangle p = 2\gamma H = \frac{4\gamma \cos\theta}{d} \quad (2)$$

Here, γ represents the interfacial tension, H is the curvature of the interface, θ is the contact angle between the interface and the pore wall, and d is the pore diameter. By analyzing the distribution of these pressure differences, the pore size distribution of the membrane can be determined.

2.3.1.1. Liquid displacement method

The liquid displacement method, based on the Young-Laplace equation, includes the bubble point method, the gas-liquid displacement method, and the liquid-liquid displacement method.

The bubble point method involves gradually increasing the pressure in all pores filled with liquid until the liquid is displaced by gas. The first pore completely displaced by gas (the first bubble) is assumed to be the largest pore in the membrane. Thus, the bubble point method is commonly used as a commercial tech-

nique to assess membrane integrity rather than to determine pore size distribution (i.e., to verify whether the pore sizes fall within the acceptable range)[11-14]. However, a drawback of this method is that high pressure is required if the gas-liquid interfacial tension is high. For instance, when using water as the wetting fluid, the water-gas interfacial tension is 73 mN/m, and approximately 15 bar of pressure is needed to analyze membranes with pore sizes up to 0.2 μm[13]. If the pressure is too high, it may deform the membrane structure, reducing measurement accuracy, so lower-tension liquids (e.g., halogenated fluids) are often used for analysis[15,16].

The gas-liquid displacement method involves gradually increasing the gas pressure after the bubble point is reached, allowing smaller pores filled with liquid to be replaced by gas. By measuring the gas pressure and flow rate, the pore size distribution of the membrane can be determined. To convert the pressure and flow rate data into pore sizes, the Hagen-Poiseuille equation is applied to describe convective flow through the pores. However, if the pore size is smaller than the mean free path of the gas, the measurement may overestimate the pore density[15]. Therefore, a combination of the Hagen-Poiseuille and Knudsen models is used to correct the pore size distribution[17]. For microfiltration membranes with pore sizes ranging from 0.1 to 0.5 μm, studies have shown that simply using the Hagen-Poiseuille behavior with a liquid having a higher interfacial tension than water (73 mN/m) is sufficient[18].

The typical procedure for measuring pore size distribution using the gas-liquid displacement method involves first immersing the membrane in liquid for a set period to ensure that the liquid fills the pores completely. Then, the membrane is placed in a dead-end filtration cell, and pressure is gradually increased. Once the first bubble appears, gas begins to permeate the membrane, and the pore size is determined based on the measured gas flow rate and applied pressure. The Young-Laplace equation is used here, and the choice of wetting fluid should match the hydrophilic or hydrophobic nature of the membrane to ensure accurate pore size calculation. However, since there is no clear standard for selecting a wetting fluid, halogenated fluids—characterized by low interfacial tension, low reactivity, and low vapor pressure—are commonly used. The gas-liquid displacement method, also known as Liquid Extrusion Porometry, Flow Permporometry, or Capillary Flow Porometry, divides the pressure application into approximately 200~300 increments, producing a pore size distribution resembling a normal distribution[19-21].

The advantages of the gas-liquid displacement method include its simplicity, non-destructive nature, and ability to analyze only interconnected pores. However, limitations include: 1) The assumption that pores are cylindrical, 2) Variation in pore size distribution based on the choice of wetting fluid, and 3) Difficulty in analyzing pores smaller than 50 nm[22]. Especially when the pore shape is irregular, the cylindrical assumption (i.e., assuming no tortuosity and using membrane thickness as pore length) can lead to inaccuracies[23].

The liquid-liquid displacement method is suitable for analyzing smaller pore sizes (ca. < 50 nm) than the gas-liquid method. Similar in principle, it uses the interface of two immiscible liquids to calculate pore size distribution. Unlike the gas-liquid method, it relies solely on the Hagen-Poiseuille model to describe convective flow, allowing for calculation of both pore numbers and sizes without the interference seen in gas-liquid behavior[24-26]. Additionally, because the liquid-liquid interfacial tension is lower than that of gas-liquid, it allows for analysis at relatively lower pressures[27].

In the liquid-liquid displacement method, two immiscible liquids are used: one acts as the wetting fluid, while the other (the displacing liquid) has low affinity with the membrane, displacing the wetting fluid from the pores. Similar to the bubble point method, when the displacing liquid begins to displace the wetting liquid at the threshold pressure, pore size is determined based on the flow rate and applied pressure. Using the Hagen-Poiseuille model, the flow rate (J_n) at each pressure step (P_n) is expressed as follows[23]:

$$J_n = \frac{\pi N_n r_n^4 P_n}{8\eta l} \quad (3)$$

where r_n is the pore diameter at step n, N_n is the number of pores at step n, η is the dynamic viscosity of the displacing fluid, and l is the pore length.

The choice and combination of wetting and displacing liquids determine the effectiveness of the liquid-liquid displacement method. Initially, water-alcohol mixtures (e.g., butanol or propanol) with low interfacial tension (ca. 1.73 mN/m) were used[27,28]. However, alcohols tend to adsorb within polymeric membranes, causing swelling and reducing measurement accuracy [29]. Recently, ammonium sulfate solution (displacing fluid) and polyethylene glycol solution (wetting fluid) have been used to prevent membrane swelling[31]. Using water-soluble polymers and salts in aqueous systems offers the advantage of easy removal after analysis, but this method is limited to hydrophilic membranes and may lack reproducibility for smaller pore sizes due to the higher viscosity of both fluids compared to water[30-32].

To improve reproducibility, the displacing and wetting liquids in the liquid-liquid displacement method should possess the following characteristics: 1) Low liquid-liquid interfacial tension, 2) Low viscosity and vapor pressure, and 3) Low adsorption within the membrane material.

The liquid-liquid displacement method's advantages include being a non-destructive analysis, targeting only interconnected pores, and its applicability to ultrafiltration and nanofiltration membranes (pore size 1~10 nm)[33]. However, the method's limitations are: 1) The assumption of cylindrical pore shapes, and 2) The lack of a clear standard for selecting wetting and displacing liquids.

2.3.2. Kelvin equation

The Kelvin equation, similar to the Young-Laplace equation, describes the interface between two immiscible fluids but focuses on the thermodynamic equilibrium when the two fluids are in contact. As shown in

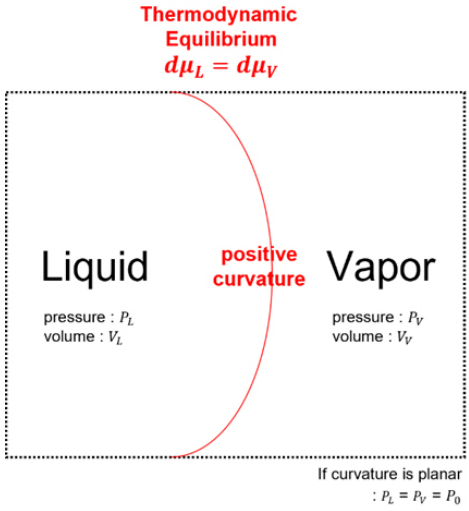

Fig. 5. Thermodynamic equilibrium of two fluids in the Kelvin Equation.

Fig. 5, when the meniscus of the liquid phase is convex toward the gas phase, the thermodynamic equilibrium between the two phases can be expressed as follows:

$$V_L(P_L - P_0) = RT\ln\frac{P_V}{P_0} \quad (4)$$

Rearranging Equation 4, it can be expressed as:

$$V_L(P_L - P_V) - V_L(P_0 - P_V) = RT\ln\frac{P_V}{P_0} \quad (5)$$

By neglecting $V_L(P_0 - P_V)$ and substituting the Young-Laplace equation into Equation 5, the Kelvin equation is derived as follows:

$$\frac{2V_L\gamma\cos\theta}{RTr} = \ln\frac{P_V}{P_0} \quad \text{or} \quad r = \frac{2V_L\gamma\cos\theta}{RT\ln\frac{P_V}{P_0}} \quad (6)$$

2.3.2.1. Permporometry

Permporometry, based on the Kelvin equation, involves reducing the gas pressure below the saturation vapor pressure so that a condensable gas fills the membrane's pores. The pressure is then gradually increased, causing the condensed gas in the pores to

evaporate, and the flow rate of a non-condensable gas like helium, nitrogen, or oxygen is used to map the pore size distribution[34,35]. In typical setups, nitrogen and the condensable gas permeate from both the feed and permeate sides of the membrane, while oxygen is sent to the permeate side to measure flow rates using gas chromatography[36].

Condensable gas, such as methanol, ethanol, propanol, or hexane, must meet two criteria: 1) It should be a wetting and inert gas, and 2) It must have suitable vapor pressure and evaporation rates for precise analysis[37,38].

Permporometry is commonly used for ceramic membranes, measuring pore sizes from 4 to 50 nm, while its derivative, Nanopermporometry, can measure pores as small as ~0.6 nm[35,37-39]. The limitation of this method lies in the assumption that the pores are non-intersecting and cylindrical, which may differ from the actual pore size distribution. Attempts have been made to improve accuracy by introducing an invasion percolation model to refine the analysis[40,41].

2.3.2.2. Gas adsorption-desorption

Gas adsorption-desorption is a widely used technique for analyzing the surface area and pore size distribution of not only porous membranes but also general porous materials. It has been applied to various membrane materials, including ceramics and polymers [42-45]. The experimental steps using a surface area analyzer (BET method) are as follows: 1) The membrane sample is thoroughly dried, 2) Helium gas is introduced at cryogenic temperatures to measure the dead volume of each test and reference cell, after which the helium is evacuated, 3) Nitrogen gas is introduced at a constant flow rate, and the pressure is monitored over time to determine the adsorption-desorption isotherm of the sample[46].

Pores are classified into three categories: macropores (pore size > 50 nm), mesopores (pore size: 2~50 nm), and micropores (pore size < 2 nm). The behavior and interpretation of the adsorption-desorption isotherm depend on the pore type. Analyzing macropores or micropores in membranes using this method can lead to measurement errors. Specifically, micropores cannot be explained by the Kelvin equation because the meniscus inside these pores does not form continuously[47]. Therefore, the gas adsorption-desorption method is best suited for mesoporous membranes, such as those used in ultrafiltration. The hysteresis observed in the adsorption-desorption isotherm may cause discrepancies between the actual and measured pore size distributions, often due to intersecting pores within the membrane [48].

2.3.2.3. Evapoporometry

Evapoporometry involves filling the membrane pores with a highly volatile wetting fluid and then gradually evaporating it while measuring the membrane weight in real-time to determine the pore size distribution[49-51]. To ensure measurement precision, the external environment must be temperature and humidity controlled [49]. The wetting fluid evaporates from larger to smaller pores, and common fluids include acetone, ethanol, isopropyl alcohol, and butanol. The effectiveness and precision of this method depend on the chemical properties of the wetting fluid. The preferred wetting fluids are those that: 1) have high volatility (or high vapor pressure), and 2) possess high interfacial tension and molar volume[51].

Evapoporometry has been reported mainly for analyzing polymeric membranes such as PES, PC, and PVDF with pore size distributions of approximately 20~100 nm. This technique can analyze both open and closed pores simultaneously, as it varies the behavior of evaporation by filling closed pores with a non-volatile, non-wetting fluid (e.g., silicone oil). The difference in the rate of evaporation over time then correlates with changes in pore size distribution[49-52]. Therefore, the results of evapoporometry depend on whether non-volatile and non-wetting fluids are used, and the method should be adapted according to the membrane material and pore characteristics.

The advantages of evapoporometry include its non-destructive nature, the ability to analyze both open

Table 1. Comparison of Microporous Membranes Pore Characterization Methods

Equation	Method	Pore size	Characteristics	Limitation
Young-Laplace Equation	Gas-liquid Displacement	r > 50 nm (Open / closed pores)	1) Pore size distribution calculated based on volume 2) Analysis possible in relatively short time	Membrane break down under high pressure
	Liquid-Liquid Displacement	r > 1 nm (Open pores)		Only ultrafiltration membranes can be analyzed
Kelvin Equation	Permporometry	r > 0.6 nm (Open pores only)	Pore size calculated based on flux	Affected by pore shape
	Gas adsorption-desorption	r > 2 nm (Open/ closed pores)	Pore size calculated based on volume	Appropriate for mesopore
	Evapoporometry	r > 5 nm (Open pores only)	1) Pore size distribution calculated based on mass 2) Analysis possible under room temperature and atmosphere	Closed pores effect on result
Gibbs-Thomson Equation	Thermoporometry	r > 3 nm (Open pores only)	Pore size distribution calculated based on mass	Calorimeter detection limits

and closed pores, and its applicability to ultrafiltration and nanofiltration membranes (pore sizes 1~10 nm). However, limitations include: 1) The assumption of cylindrical pores, and 2) The lack of clear criteria for selecting the appropriate wetting and displacing fluids.

2.3.3. Gibbs-Thomson equation

While the Kelvin equation explains thermodynamic equilibrium under isothermal conditions through pressure variations, the Gibbs-Thomson equation describes thermodynamic equilibrium under isobaric conditions, focusing on temperature changes. When a liquid confined in pores solidifies at low temperatures, the free energy at the liquid-solid interface changes. This can be expressed as a function of phase transition temperature (T) as follows[53,54]:

$$T = T_0 - \int_{T}^{T_0} \frac{V_L}{\Delta S_F} d(\gamma_{ls} C_{ls}) \tag{7}$$

Here, T_0 is the initial temperature, V_L is the molar volume of the liquid, ΔS_F is the heat of fusion, γ_{ls} is the liquid-solid interfacial tension, and C_{ls} is the curvature of the liquid-solid interface. The solid formed from the liquid, whether as a meniscus or a spherical nucleus due to nucleation, has the following curvature:

$$C_{ls} = \frac{2}{(r-t)} \tag{8}$$

where r is the pore diameter, and t is the thickness of the condensate layer that adheres to the pore wall and does not participate in the phase transition. Combining Equations 7 and 8 allows for determining pore size as a function of temperature variation. For instance, if benzene is used as the liquid, the equation becomes [54]:

$$r[nm] = -\frac{131.6}{\Delta T} + 0.54 \tag{9}$$

2.3.3.1. Thermoporometry

Thermoporometry is a technique capable of analyzing pore sizes in the range of 3~300 nm. While it has not been extensively reported for membrane pore analysis, it has primarily been applied to polymer materials such as polysulfone (PSF) and polycarbonate (PC) [55-57]. The pore size distribution is plotted based on phase transition curves obtained using calorimetry. The sample is soaked in a liquid, frozen, and then gradually thawed while monitoring the change in heat. Benzene or water is typically used as the fluid because these solvents facilitate observation of freezing-melting conditions in calorimetry setups.

3. Conclusions

Membranes can be considered a type of black box, where the membrane medium is continuously influenced by the physicochemical properties of the permeating species, and, in turn, the diffusion behavior of the permeating species is dynamically affected by the membrane. In porous membranes, the diffusion pathways (pores) are formed irregularly within the membrane matrix, making it challenging to define boundary conditions. This paper reviews analytical techniques that can standardize and infer these irregular pore characteristics. The most commonly reported and preferred methods for determining pore size distribution are based on the Young-Laplace equation, Kelvin equation, and Gibbs-Thomson equation, with liquid displacement methods and evapoporometry being particularly prevalent. The features and limitations of each method are summarized in Table 1.

A common limitation of these techniques is that they assume the pores are cylindrical, which may not accurately represent the actual pore structure and characteristics. Additionally, none of these methods provide a definitive criterion for selecting the fluid used to fill the pores. Since the pore characteristics of membranes depend on the properties of the wetting fluid (e.g., wettability, calorific value, interfacial tension), it is important to choose the appropriate fluid and analytical method based on the membrane's material, structure, and properties. Furthermore, the results of pore characteristic analysis should be cross-validated with other techniques such as SEM and AFM to ensure accuracy.

Acknowledgments

This work was supported by the Materials & Components Technology Development Program (Project number: 20011497) funded by the Ministry of Trade, Industry & Energy (MOTIE, Korea).

Reference

1. G. Owen, M. Bandi, J. A. Howell, and S. J. Churchouse, "Economic assessment of membrane processes for water and wastewater treatment", *J. Membr. Sci.*, **102**, 77-91 (1995).
2. H. D. Lee, Y. H. Cho, and H. B. Park, "Current research trends in water treatment membranes based on nano materials and nano technologies", *Membr. J.*, **23**, 101-111 (2013).
3. R. W. Baker, "Membrane technology and applications", John Wiley & Sons, Chichester, West Sussex (2012).
4. E. M. Renkin, "Filtration, diffusion, and molecular sieving through porous cellulose membranes", *J. Gen. Physiol.*, **38**, 225 (1954).
5. R. W. Baker and H. Strathmann, "Ultrafiltration of macromolecular solutions with high-flux membranes", *J. Appl. Polym. Sci.*, **14**, 1197-1214 (1970).
6. R. Singh, "Hybrid membrane systems for water purification: Technology, systems design and operations", Elsevier, Amsterdam, The Netherlands (2006).
7. I. Park, J. H. Kang, Y. Ha, J. Lee, and H. B. Park, "Hydrothermally rearranged cellulose membranes for controlled size sieving", *J. Membr. Sci.*, **173**, 123367 (2025).
8. J. I. Calvo, A. Bottino, G. Capannelli, and A. Hernández, "Comparison of liquid–liquid displacement porosimetry and scanning electron microscopy image analysis to characterise ultrafiltration track-etched membranes", *J. Membr. Sci.*, **239**, 189-197 (2004).
9. R. Ziel, A. Haus, and A. Tulke, "Quantification of the pore size distribution (porosity profiles) in microfiltration membranes by SEM, TEM and computer image analysis", *J. Membr. Sci.*, **323**, 241-246 (2008).
10. N. A. Ochoa, P. Pradanos, L. Palacio, C. Pagliero, J. Marchese, and A. Hernández, "Pore size distributions based on AFM imaging and retention of multidisperse polymer solutes: Characterisation of polyethersulfone UF membranes with dopes con-

taining different PVP", *J. Membr. Sci*., **187**, 227-237 (2001).
11. G. Reichelt, "Bubble point measurements on large areas of microporous membranes", *J. Membr. Sci*., **60**, 253-259 (1991).
12. E. Jakobs and W. Koros, "Ceramic membrane characterization via the bubble point technique", *J. Membr. Sci*., **124**, 149-159 (1997).
13. D. Hopkinson, M. Zeh, and D. Luebke, "The bubble point of supported ionic liquid membranes using flat sheet supports", *J. Membr. Sci.*, **468**, 155-162 (2014).
14. H. Bechhold, "Durchlässigkeit von ultrafiltern", *Z. Phys. Chem.*, **64**, 328-342 (1908).
15. A. Hernández, J. Calvo, P. Prádanos, and F. Tejerina, "Pore size distributions in microp- orous membranes. A critical analysis of the bubble point extended method", *J. Membr. Sci.*, **112**, 1-12 (1996).
16. R. I. Peinador, J. I. Calvo, and R. Ben Aim, "Comparison of capillary flow porometry (CFP) and liquid extrusion porometry (LEP) techniques for the characterization of porous and face mask membranes", *Appl. Sci.*, **10**, 5703 (2020).
17. P. Shao, R. Huang, X. Feng, and W. Anderson, "Gas-liquid displacement method for estimating membrane pore-size distributions", *AIChE J.*, **50**, 557-565 (2004).
18. R. I. Peinador, O. Abba, and J. I. Calvo, "Characterization of commercial gas diffusion layers (GDL) by liquid extrusion porometry (LEP) and gas liquid displacement porometry (GLDP)", *Membranes*, **12**, 212 (2022).
19. R. Mourhatch, T. T. Tsotsis, and M. Sahimi, "Determination of the true pore size distribution by flow permporometry experiments: an invasion percolation model", *J. Membr. Sci.*, **367**, 55-62 (2011).
20. D. Li, M. W. Frey, and Y. L. Joo, "Characterization of nanofibrous membranes with capillary flow porometry", *J. Membr. Sci.*, **286**, 104-114 (2006).
21. H. Kolb, R. Schmitt, A. Dittler, and G. Kasper, "On the accuracy of capillary flow porometry for fibrous filter media", *Sep. Purif. Technol.*, **199**, 198-205 (2018).
22. D. Dollimore and G. Heal, "An improved method for the calculation of pore size distribution from adsorption data", *J. Appl. Chem.*, **14**, 109-114 (1964).
23. R. I. Peinador, J. I. Calvo, P. Prádanos, L. Palacio, and A. Hernández, "Characterisation of polymeric UF membranes by liquid–liquid displacement porosimetry", *J. Membr. Sci.*, **348**, 238-244 (2010).
24. G. Capannelli, F. Vigo, and S. Munari, "Ultrafiltration membranes—characterization methods", *J. Membr. Sci.*, **15**, 289-313 (1983).
25. S Munari, A. Bottino, G. Capannelli, and P. Moretti, "Membrane morphology and transport properties", *Desalination*, **53**, 11-23 (1985).
26. M. B. Tanis-Kanbur, R. I. Peinador, X. Hu, J. I. Calvo, and J. W. Chew, "Membrane characterization via evapoporometry (EP) and liquid-liquid displacement porosimetry (LLDP) techniques", *J. Membr. Sci.*, **586**, 248-258 (2019).
27. P. Grabar and S. Nikitine, "Sur le diamètre des pores des membranes en collodion utilisèes en ultrafiltration", *J. Chim. Phys.*, **33**, 721-741 (1936).
28. J. I. Calvo, R. I. Peinador, P. Prádanos, L. Palacio, A. Bottino, G. Capannelli, and A. Hernández, "Liquid–liquid displacement porometry to estimate the molecular weight cut-off of ultrafiltration membranes", *Desalination*, **268**, 174-181 (2011).
29. L. Germic, K. Ebert, R. Bouma, Z. Borneman, M. Mulder, and H. Strathmann, "Characterization of polyacrylonitrile ultrafiltration membranes", *J. Membr. Sci.*, **132**, 131-145 (1997).
30. S. M. Snyder, K. D. Cole, and D. C. Szlag, "Phase compositions, viscosities, and densities for aqueous two-phase systems composed of polyethylene glycol and various salts at 25. degree. C", *J. Chem. Eng. Data*., **37**, 268-274 (1992).
31. M. W. Phillips and A. J. DiLeo, "A validatible porosimetric technique for verifying the integrity of virus-retentive membranes", *Biologicals*., **24**, 243-253 (1996).
32. S. Giglia, D. Bohonak, P. Greenhalgh, and A.

Leahy, “Measurement of pore size distribution and prediction of membrane filter virus retention using liquid–liquid porometry”, *J. Membr. Sci.*, **476**, 399-409 (2015).
33. P. Carretero, S. Molina, A. Lozano, J. de Abajo, J. I. Calvo, P. Prádanos, L. Palacio, and A. Hernández, “Liquid–liquid displacement porosimetry applied to several MF and UF membranes”, *Desalination*, **327**, 14-23 (2013).
34. F. P. Cuperus, D. Bargeman, and C. A. Smolders, “Permporometry: The determination of the size distribution of active pores in UF membranes”, *J. Membr. Sci.*, **71**, 57-67 (1992).
35. T. Tsuru, Y. Takata, H. Kondo, F. Hirano, T. Yoshioka, and M. Asaeda, “Characterization of sol –gel derived membranes and zeolite membranes by nanopermporometry”, *Sep. Purif. Technol.*, **32**, 23-27 (2003).
36. G. Cao, J. Meijernik, H. Brinkman, and A. Burggraaf, “Permporometry study on the size distribution of active pores in porous ceramic membranes”, *J. Membr. Sci.*, **83**, 221-235 (1993).
37. T. Tsuru, T. Hino, T. Yoshioka, and M. Asaeda, “Permporometry characterization of microporous ceramic membranes”, *J. Membr. Sci.*, **186**, 257-265 (2001).
38. P. Huang, N. Xu, J. Shi, and Y. Lin, “Characterization of asymmetric ceramic membranes by modified permporometry”, *J. Membr. Sci.*, **116**, 301-305 (1996).
39. A. Simon, H. Richter, B. Reif, M. Schuelein, D. Sanwald, and W. Schwieger, “Evaluation of a method for micro-defect sealing in ZSM-5 zeolite membranes by chemical vapor deposition of carbon”, *Sep. Purif. Technol.*, **219**, 180-185 (2019).
40. S. Blumenschein, A. Böcking, U. Kätzel, S. Postel, and M. Wessling, “Rejection modeling of ceramic membranes in organic solvent nanofiltration”, *J. Membr. Sci.*, **510**, 191-200 (2016).
41. S. Zeidler, P. Puhlfürß, U. Kätzel, and U. I. Voigt, “Preparation and characterization of new low MWCO ceramic nanofiltration membranes for organic solvents”, *J. Membr. Sci.*, **470**, 421-430 (2014).
42. D. Korelskiy, M. Grahn, J. Mouzon, and J. Hedlund, “Characterization of flow-through micropores in MFI membranes by permporometry”, *J. Membr. Sci.*, **417**, 183-192 (2012).
43. A. K. Basumatary, R. V. Kumar, A. K. Ghoshal, and G. Pugazhenthi, “Synthesis and characterization of MCM-41-ceramic composite membrane for the separation of chromic acid from aqueous solution”, *J. Membr. Sci.*, **475**, 521-532 (2015).
44. W. Oh and J-W. Park, “Facile synthesis of robust and pore-size-tunable nanoporous covalent framework membrane by simultaneous gelation and phase separation of covalent network/poly (methyl methacrylate) mixture”, *ACS Appl. Mater. Interfaces.*, **11**, 32398-32407 (2019).
45. Z. Ashrafi, L. Lucia, and W. Krause, “Bioengineering tunable porosity in bacterial nanocellulose matrices”, *Soft Matter*, **15**, 9359-9367 (2019).
46. P. Prádanos, M. L. Rodriguez, J. Calvo, A. Hernández, F. Tejerina, and J. De Saja, “Structural characterization of an UF membrane by gas adsorption-desorption and AFM measurements”, *J. Membr. Sci.*, **117**, 291-302 (1996).
47. K. Kaneko, “Determination of pore size and pore size distribution: 1. Adsorbents and catalysts”, *J. Membr. Sci.*, **96**, 59-89 (1994).
48. F. Cuperus and C. Smolders, “Characterization of UF membranes: Membrane characteristics and characterization techniques”, *Adv. Colloid Interface Sci.*, **34**, 135-173 (1991).
49. W. B. Krantz, A. R. Greenberg, E. Kujundzic, A Yeo, and S. S. Hosseini, “Evapoporometry: A novel technique for determining the pore-size distribution of membranes”, *J. Membr. Sci.*, **438**, 153-166 (2013).
50. E. Akhondi, F. Wicaksana, W. B. Krantz, and A. G. Fane, “Evapoporometry determination of pore-size distribution and pore fouling of hollow fiber membranes”, *J. Membr. Sci.*, **470**, 334-345 (2014).
51. F. Zamani, P. Jayaraman, E. Akhondi, W. B. Krantz, A. G. Fane, and J. W. Chew, “Extending

the uppermost pore diameter measureable *via* Evapoporometry", *J. Membr. Sci.*, **524**, 637-643 (2017).
52. M. B. Tanis-Kanbur, F. Zamani, W. B. Krantz, X. Hu, and J. W. Chew, "Adaptation of evapoporometry (EP) to characterize the continuous pores and interpore connectivity in polymeric membranes", *J. Membr. Sci.*, **575**, 17-27 (2019).
53. M. Brun, A. Lallemand, J-F. Quinson, and C. Eyraud, "A new method for the simultaneous determination of the size and shape of pores: the thermoporometry", *Thermochim. Acta*, **21**, 59-88 (1977).
54. J. Quinson, N. Mameri, L. Guihard, and B. Bariou, "The study of the swelling of an ultrafiltration membrane under the influence of solvents by thermoporometry and measurement of permeability", *J. Membr. Sci.*, **58**, 191-200 (1991).
55. L. Zeman, G. Tkacik, and P. Le Parlouer, "Characterization of porous sublayers in UF membranes by thermoporometry", *J. Membr. Sci.*, **32**, 329-337 (1991).
56. C. Jallut, J. Lenoir, C. Bardot, and C. Eyraud, "Thermoporometry.: Modelling and simulation of a mesoporous solid", *J. Membr. Sci.*, **68**, 271-282 (1992).
57. F. Cuperus, D. Bargeman, and C. Smolders, "Critical points in the analysis of membrane pore structures by thermoporometry", *J. Membr. Sci.*, **66**, 45-53 (1992).